Multibaseline Two Layer Model PolInSAR Ground and Volume Separation

Alberto Alonso-González, German Aerospace Center (DLR), alberto.alonso-gonzalez@dlr.de, Germany
Kostas P. Papathanassiou, German Aerospace Center (DLR), kostas.papathanassiou@dlr.de, Germany

Abstract

This work introduces a method to separate the ground and volume contributions from Polarimetric SAR Interferometric acquisitions. Based on the two layer model, the radar response may be decomposed into these two main components and the full rank polarimetric covariance matrices of the corresponding ground and volume layers may be extracted from the data. The technique is evaluated with real multibaseline fully polarimetric L-band data acquired in 2009 by the E-SAR airborne sensor over the forest in Traunstein, southern Germany.

1 Introduction

Polarimetric SAR Interferometry combines the advantage of polarimetric diversity, in order to discriminate between different scatterers within the resolution cell, with interferometry, allowing sensitivy to the vertical dimension and its distribution.
Coherent PolInSAR scattering models based on two layers, corresponding to the ground and the vegetation, have been used traditionally to extract forest biophysical parameters [1][2]. This paper, however, deals with the separation of the radar response of the ground and volume components based on this model. Additionally, multiple baseline information will be combined under the model framework in order to improve characterization accuracy and remove inversion ambiguities.

2 PolInSAR Two Layer Model

Multibaseline PolInSAR sensors measure the fully polarimetric response of the target at N different baselines. In this context the Multipolarization Multibaseline covariance matrix $\mathbf{T}_N$ may be expressed as

$$\mathbf{T} = \langle \mathbf{k}\mathbf{k}^H \rangle = \begin{pmatrix} \mathbf{T}_{11} & \mathbf{\Omega}_{12} & \cdots & \mathbf{\Omega}_{1N} \\ \mathbf{\Omega}_{12}^H & \mathbf{T}_{22} & \cdots & \mathbf{\Omega}_{2N} \\ \vdots & \vdots & \ddots & \vdots \\ \mathbf{\Omega}_{1N}^H & \mathbf{\Omega}_{2N}^H & \cdots & \mathbf{T}_{NN} \end{pmatrix} \tag{1}$$

$$\mathbf{k} = \left[\mathbf{k}_1^T \mathbf{k}_2^T \cdots \mathbf{k}_N^T \right]^T \tag{2}$$

$$\mathbf{k}_i = \frac{1}{\sqrt{2}} \left[\; S_{hh}^i + S_{vv}^i, \quad S_{hh}^i - S_{vv}^i, \quad S_{hv}^i + S_{vh}^i \; \right]^T. \tag{3}$$

Traditionally, two layer models have been widely used in SAR polarimetry and interferometry to describe the radar response in vegetation scenarios. In these models the target is decomposed into two main physical components: the soil, considered as an impenetrable surface, and the vegetation on top of it, represented by a volume of small scatterers. Two layer models have been also employed for interferometry as, for instance, the Random Volume Over Ground (RVOG) [2] or the interferometric water cloud model (IWM) [1].
According to the two layer model, the interferometric coherence γ_{ij} between acquisition i and j for a particular polarization state $\mathbf{w}$ may be expressed as [2]

$$\gamma_{ij}(\mathbf{w}) = \frac{\mathbf{w}^H \mathbf{\Omega}_{ij} \mathbf{w}}{\sqrt{\mathbf{w}^H \mathbf{T}_{ii} \mathbf{w} \cdot \mathbf{w}^H \mathbf{T}_{jj} \mathbf{w}}} = \frac{\gamma_{ij}^v + \gamma_{ij}^g \mu(\mathbf{w})}{1 + \mu(\mathbf{w})} \tag{4}$$

where γ_{ij}^g and γ_{ij}^v represent the interferometric coherence for the ground and volume layers, respectively, defined as

$$\gamma_{ij}^l = \frac{\int F^l(z) e^{j k_{z_{ij}} z} \, dz}{\int F^l(z) \, dz}, \tag{5}$$

with $l \in (g, v)$, $k_{z_{ij}}$ is the vertical wavenumber between acquisition i and j, and $\mu(w)$ represents the ground to volume power ratio for the polarization state $\mathbf{w}$

$$\mu(\mathbf{w}) = \frac{\mathbf{w}^H \mathbf{T}_g \mathbf{w}}{\mathbf{w}^H \mathbf{T}_v \mathbf{w}}. \tag{6}$$

Equations (4)-(6) encapsulate the two basic assumptions of the two layer model:

1. The vertical profiles $F^g(z)$ and $F^v(z)$ do not depend on $\mathbf{w}$, resulting into ground and volume coherences γ_{ij}^g and γ_{ij}^v independent of the polarization state.

2. The vertical profiles $F^g(z)$ and $F^v(z)$ and ground and volume responses $\mathbf{T}_g$ and $\mathbf{T}_v$ do not depend on the acquisition, that is, they are constant.

As mentioned in [2], under these assumptions the coherence region for each baseline $\gamma_{ij}(\mathbf{w})$ is following a line between the two layers coherences γ_{ij}^g and γ_{ij}^v controlled by the ground to volume ratio $\mu(\mathbf{w})$. Different two layer models differ only in the interpretation of these layers or their vertical profile $F^l(z)$ definition, but the coherence line and the previous conclusions are always obtained regardless the choice of the vertical profile function.

3 Ground and Volume Response Separation

It is worth mentioning that (4) indirectly separates the polarimetric and interferometric components into the $\mu(\mathbf{w})$ and γ_{ij}^{g}, γ_{ij}^{v} factors, respectively. This allows one to define the different coherence $\mathbf{T}_{ii}$ and PolInSAR $\mathbf{\Omega}_{ij}$ matrices in (1) as already noted in [3] [4]

$$\mathbf{T}_{ii} = \mathbf{T}_g + \mathbf{T}_v \tag{7}$$

$$\mathbf{\Omega}_{ij} = \gamma_{ij}^{g}\mathbf{T}_g + \gamma_{ij}^{v}\mathbf{T}_v \tag{8}$$

In the multibaseline approach, the representation of the two layer models covariance matrix $\mathbf{T}$ defined in (1) may be expressed by a Sum of Kronecker Products (SKP), as described in [6]

$$\mathbf{T} = \mathbf{R}_g \otimes \mathbf{T}_g + \mathbf{R}_v \otimes \mathbf{T}_v \tag{9}$$

where $\mathbf{R}_g$ and $\mathbf{R}_v$ represent the structure matrices of the ground and volume, respectively.

Equations (9) and (7), (8) show that it is possible to extract the ground and volume coherence matrices $\mathbf{T}_g$ and $\mathbf{T}_v$ knowing the ground and volume coherences γ_{ij}^{g} and γ_{ij}^{v}. Then, the issue is the estimation of the appropriate ground and volume coherences from the data, which is not straightforward. On the one hand, the position of γ^g and γ^v over the line is ambiguous, as already discussed in [2], resulting into different values for $\mathbf{T}_g$ and $\mathbf{T}_v$. This problem is usually solved by making an assumption to remove the ambiguity, like $\mu_{min} = 0$. These assumptions, however, are not generally true and may bias the obtained ground and volume components. On the other hand, algebraic decompositions like the SKP find the components that minimize the error in the Frobenius norm. In the presence of speckle, due to its multiplicative nature, this may pose a problem when the power difference of the 2 components is relatively large (which is commonly the case) as one of the components may fall within the noise level. Moreover, since it is not a model-based approach, the obtained results are more difficult to interpret physically. To solve these problems, some hybrid decompositions have been proposed [7] [5].

In this work a different approach is proposed. A fully model-based approach is employed but trying to avoid any a priori assumptions over $\mu(\mathbf{w})$ by combining the multiple baseline acquisitions information. As mentioned before, $\mu(\mathbf{w})$ depends only on the polarimetric response on the target which is, therefore, assumed to be constant over the different baselines. In matrix notation μ will be represented by the matrix $\mathbf{M}$, defined according to (4) and (6) as

$$\mathbf{M} = \mathbf{T}_{vn}^{-1}\mathbf{T}_{gn} = \left(\gamma_{ij}^{v}\mathbf{I} - \mathbf{\Pi}_{ij}\right)\left(\mathbf{\Pi}_{ij} - \gamma_{ij}^{g}\mathbf{I}\right)^{-1} \tag{10}$$

$$\mathbf{\Pi}_{ij} = \mathbf{T}_{ii}^{-\frac{1}{2}}\mathbf{\Omega}_{ij}\mathbf{T}_{jj}^{-\frac{1}{2}}. \tag{11}$$

Note that in (10) and (11) a polarimetric prewhitening filter has been applied in order to obtain the interferometric coherences as the numerical range of the $\mathbf{\Pi}_{ij}$ matrices [4]

$$\tilde{\mathbf{T}} = \mathbf{N}_T^{-\frac{1}{2}}\mathbf{T}\mathbf{N}_T^{-\frac{1}{2}} = \begin{pmatrix} \mathbf{I} & \mathbf{\Pi}_{12} & \cdots & \mathbf{\Pi}_{1N} \\ \mathbf{\Pi}_{12}^H & \mathbf{I} & \cdots & \mathbf{\Pi}_{2N} \\ \vdots & \vdots & \ddots & \vdots \\ \mathbf{\Pi}_{1N}^H & \mathbf{\Pi}_{2N}^H & \cdots & \mathbf{I} \end{pmatrix} \tag{12}$$

$$\mathbf{N}_T = \begin{pmatrix} \mathbf{T}_{11} & \mathbf{0} & \cdots & \mathbf{0} \\ \mathbf{0} & \mathbf{T}_{22} & \cdots & \mathbf{0} \\ \vdots & \vdots & \ddots & \vdots \\ \mathbf{0} & \mathbf{0} & \cdots & \mathbf{T}_{NN} \end{pmatrix} \tag{13}$$

The prewhitening defined in (12) allows for slightly different $\mathbf{T}_{ii}$ polarimetric matrices, as occurring in real data. Additionally, it also affects (7) and (8) which may be rewritten as

$$\mathbf{T}_{ii} = \mathbf{T}_{ii}^{\frac{1}{2}}\left(\mathbf{T}_{gn} + \mathbf{T}_{vn}\right)\mathbf{T}_{ii}^{\frac{1}{2}} \tag{14}$$

$$\mathbf{I} = \mathbf{T}_{gn} + \mathbf{T}_{vn} \tag{15}$$

$$\mathbf{\Pi}_{ij} = \gamma_{ij}^{g}\mathbf{T}_{gn} + \gamma_{ij}^{v}\mathbf{T}_{vn} \tag{16}$$

where $\mathbf{T}_{gn}$ and $\mathbf{T}_{vn}$ are the prewhitened, according to (12), ground and volume covariance matrices. Note that the assumption of constant ground to volume ratio $\mathbf{M}$ involves constant $\mathbf{T}_{gn}$ and $\mathbf{T}_{vn}$ among the different acquisitions, although $\mathbf{T}_g$ and $\mathbf{T}_v$ may be slightly different for each acquisition i after dewhitening trough (14).

3.1 Direct separation

From equations (15) and (16) it may be seen that the normalized ground and volume covariance matrices $\mathbf{T}_{gn}$ and $\mathbf{T}_{vn}$ may be extracted by knowing the ground and volume coherences

$$\mathbf{T}_{vn} = \frac{\mathbf{\Pi}_{ij} - \gamma_{ij}^{g}\mathbf{I}}{\gamma_{ij}^{v} - \gamma_{ij}^{g}} \tag{17}$$

$$\mathbf{T}_{gn} = \frac{\mathbf{\Pi}_{ij} - \gamma_{ij}^{v}\mathbf{I}}{\gamma_{ij}^{g} - \gamma_{ij}^{v}}. \tag{18}$$

Equations (17) and (18) show that, assuming the coherence lineality, fixing one of the coherences defines the covariance matrix of the other component up to a scalar factor that is inversely proportional to the distance between the ground and volume coherences. For instance, fixing the ground coherence γ_{ij}^{g} defines the covariance matrix of the volume $\mathbf{T}_{vn}$ up to a scalar factor $(1/(\gamma_{ij}^{v} - \gamma_{ij}^{g}))$. The symmetric behavior may be observed for the ground component.

3.2 Ground to volume matrix

The ground and volume components may also be extracted when the ground to volume matrix $\mathbf{M}$ is fixed, according to equations (10) and (15)

$$\mathbf{T}_{vn} = \left(\mathbf{M} + \mathbf{I}\right)^{-1} \tag{19}$$

$$\mathbf{T}_{gn} = \left(\mathbf{M}^{-1} + \mathbf{I}\right)^{-1}. \tag{20}$$

Note that, in this case, the equations do not depend on the full set of ground and volume coherences γ_{ij}^g and γ_{ij}^v since this dependence is embodied in the definition of the **M** matrix in (10).

3.3 Fixing ground and volume coherences

As it may be seen in the precious sections, in order to estimate the ground and volume covariance matrices, the set of ground and volume coherences γ_{ij}^g and γ_{ij}^v need to be defined for all the baselines. In order to solve this problem, a parametric model needs to be defined for the ground and volume vertical profiles $F^g(z, \mathbf{\Phi}_g)$ and $F^v(z, \mathbf{\Phi}_v)$. Therefore, the ground and volume profiles are defined by some parameters represented by $\mathbf{\Phi}_g$ and $\mathbf{\Phi}_v$. Note that this step is required in order to link the ground and volume coherences of the different baselines through equation (5). When the total numbers of parameters required for the model are smaller than the number of baselines combinations, the problem may be solved in a least squares minimization procedure. In order to make polarimetric and interferometric components consistent, this minimization process has to be performed under the constraint of constant ground and volume components $\mathbf{T}_{gn}$ and $\mathbf{T}_{vn}$ or their ratio **M**.
In this work, the same interferometric model for the ground and volume layers than in the RVOG is applied [2]. Assuming that the different baelines have been properly phase calibrated, the vertical profile of the ground component will be assumed as a delta at h_0

$$F^g(z, h_0) = \delta(z - h_0) \tag{21}$$

$$\gamma_{ij}^g = e^{jk_{z_{ij}}h_0}. \tag{22}$$

On the other hand, the volume will be assumed as an exponential profile, starting at h_0 and with a height h_v, having an extinction parameter σ_v [2]

$$F^v(z, h_v, \sigma_v) = e^{-2\sigma_v(h_v+h_0-z)/\cos\theta} \tag{23}$$

$$\gamma_{ij}^v = \frac{2\sigma e^{jk_{z_{ij}}h_0}}{\cos\theta(e^{2\sigma h_v/\cos\theta} - 1)} \cdot \cdot \int_0^{h_v} e^{jk_{z_{ij}}z} e^{2\sigma z/\cos\theta}\, dz. \tag{24}$$

Then, with this model, the least squares minimization may be performed over the normalized multipilarization multibaselines covariance matrix $\tilde{\mathbf{T}}$

$$\text{minimize} \sum_{i,j|i\neq j} \|\mathbf{\Pi}_{ij} - \left(\gamma_{ij}^v \mathbf{T}_{vn} + \gamma_{ij}^g \mathbf{T}_{gn}\right)\|_F^2 \tag{25}$$

where $\mathbf{T}_{vn}$ and $\mathbf{T}_{gn}$ may be estimated as the all-baselines average of the hermitian part of the matrices defined in (17), (18) or (19), (20) and the ground and volume coherences γ_{ij}^g and γ_{ij}^v are defined in (22) and (24).

4 Results

In order to analyze the proposed technique, a real L-band ESAR dataset is employed. This dataset consists of 7 airborne acquisitions acquired on the 11th May 2009 over the Traunsten dataset, in southern Germany. Six different horizontal baselines where acquired with respect to the master at approximately ± 5, ± 10 and ± 15 meters. The Pauli RGB of the master acquisition may be seen on Fig. 1a. Similarly, the Pauli RGB of the obtained covariance matrices $\mathbf{T}_g$ and $\mathbf{T}_v$ for the ground and volume are represented in Fig. 1b and 1c, respectively. The areas where the model could not be inverted since they may not be described by the two layer model are represented in black.

Note that, since these are full rank covariance matrices, their polarimetric information may be analyzed more in detail. Fig. 2 shows the Entropy (H) and mean alpha parameter of the master acquisition, whereas Fig. 3 shows the same parameters for the obtained ground and volume components. The non invertible pixels are represented in white.

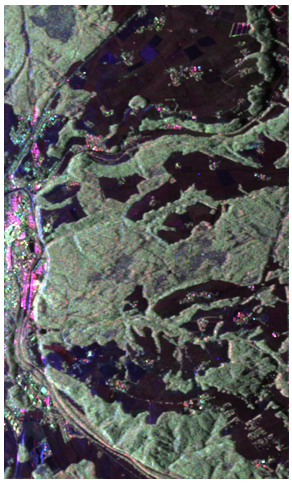

(a) Original

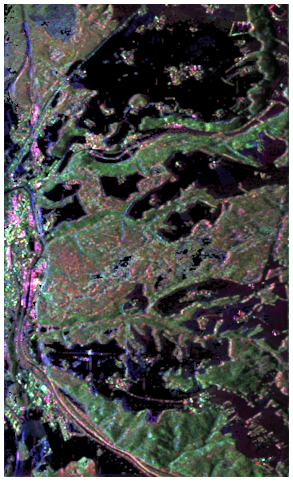

(b) Ground

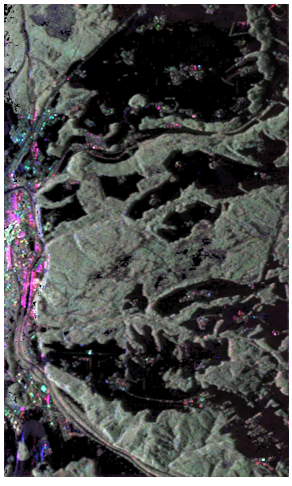

(c) Volume

Figure 1: Pauli RGB representation of the first acquisition and of the extracted ground and volume components.

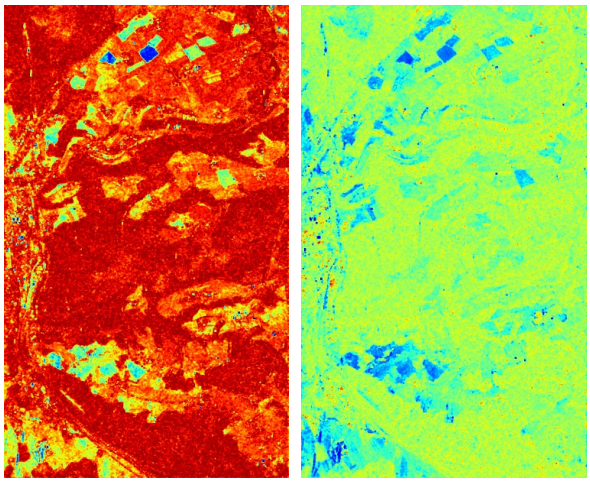

(a) H **(b)** alpha

Figure 2: Entropy (H) and mean alpha angle of the master acquisition.

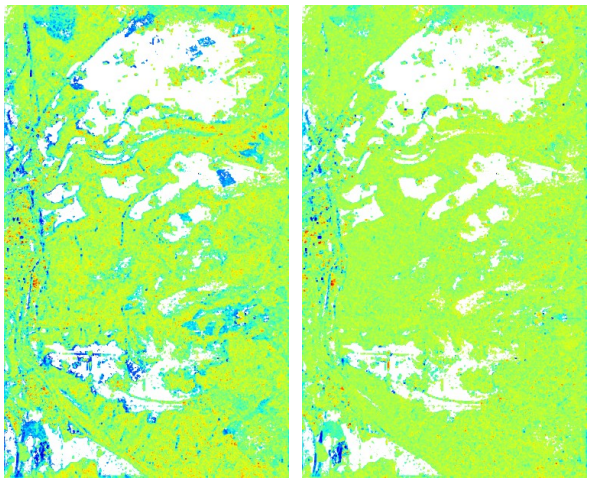

(c) alpha, $\mathbf{T}_g$ **(d)** alpha, $\mathbf{T}_v$

Figure 3: Entropy (H) and mean alpha angle of the obtained ground and volume components.

As it may be seen in Figs. 3a and 3b, significantly higher entropy is obtained for the volume component than for the ground, as one may expect from the combination of a random volume over a ground + dihedral that is usually assumed in polarimetric models. Moreover, although some details may be seen in the volume Pauli image in Fig. 1c due to variation on the backscattered power, most of these details disappear over the entropy and mean alpha parameters, shown in Figs. 3b and 3d, as one may expect in the volume layer. On the contrary, most of these details and features appear on the ground component, in Figs. 1b, 3a and 3c. Therefore this qualitative analysis shows that the obtained ground and volume components are consistent with the understanding given by physical models.

It is worth mentioning that, since this is a full model-based approach, the parameters of the model are also obtained as an outcome, for instance, forest height and volume extinction.

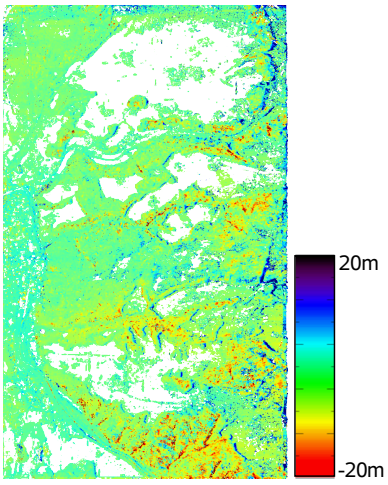

(a) h_0

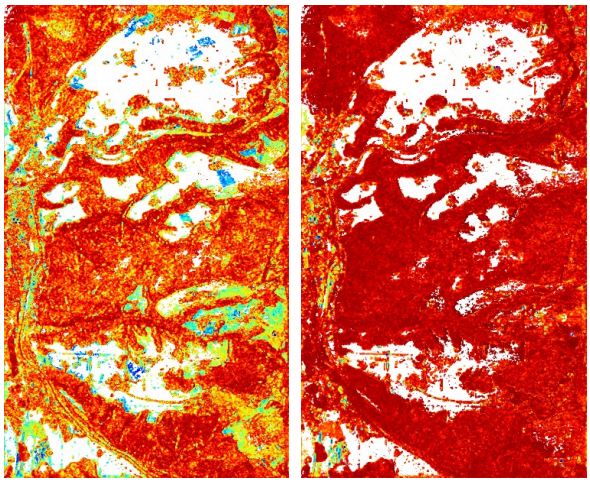

(a) H, $\mathbf{T}_g$ **(b)** H, $\mathbf{T}_v$

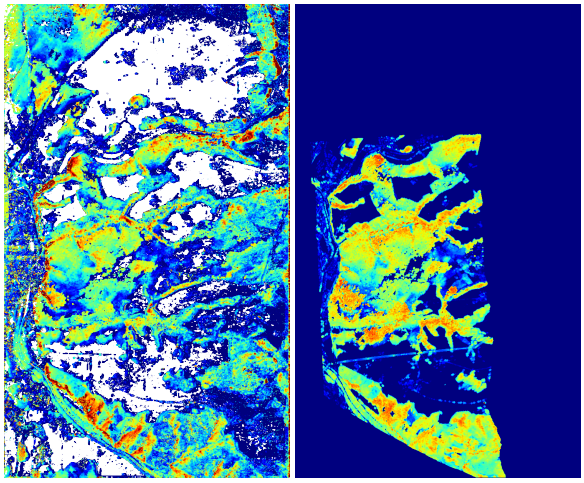

(b) h_v **(c)** lidar height

Figure 4: Estimated ground height h_0 (a) and forest height h_v (b).

References

[1] J. Askne, P.B. Dammert, L.M. Ulander, and G. Smith. C-band repeat-pass interferometric SAR observations of the forest. *IEEE Transactions on Geoscience and Remote Sensing*, 35(1):25–35, 1997.

[2] S.R. Cloude and K.P. Papathanassiou. Three-stage inversion process for polarimetric SAR interferometry. *IEE Proceedings-Radar, Sonar and Navigation*, 150(3):125–134, 2003.

[3] Y. Cui, Y. Yamaguchi, H. Yamada, and S.-E. Park. PolInSAR Coherence Region Modeling and Inversion: The Best Normal Matrix Approximation Solution. *IEEE Transactions on Geoscience and Remote Sensing*, 53(2):1048–1060, 2015.

[4] C. Lopez-Martinez and A. Alonso-Gonzalez. Assessment and estimation of the RVoG model in polarimetric SAR interferometry. *IEEE transactions on geoscience and remote sensing*, 52(6):3091–3106, 2014.

[5] M. Pardini and K. Papathanassiou. On the Estimation of Ground and Volume Polarimetric Covariances in Forest Scenarios With SAR Tomography. *IEEE Geoscience and Remote Sensing Letters*, 14(10):1860–1864, Oct 2017.

[6] S. Tebaldini. Algebraic synthesis of forest scenarios from multibaseline PolInSAR data. *IEEE Transactions on Geoscience and Remote Sensing*, 47(12):4132–4142, 2009.

[7] S. Tebaldini. Single and multipolarimetric SAR tomography of forested areas: A parametric approach. *IEEE Transactions on Geoscience and Remote Sensing*, 48(5):2375–2387, 2010.